RISET
Geologi dan Pertambangan
Indonesian Journal of Geology and Mining
https://jrisetgeotam.lipi.go.id

Research article

Carbonate rocks in northern of West Jiwo Hills Bayat: The indication of thrust belt development in southern Central Java

Ardhan Farisan[1], Muhammad Gazali Rachman[2]

[1] Research Center for Geological Resources, National Research and Innovation Agency. KST Samaun Samadikun BRIN, Bandung
[2] Geological Engineering Department, University of Pembangunan Nasional "Veteran" Yogyakarta. Jl. Padjadjaran Ring Road Utara, Condongcatur, Depok, Sleman

ABSTRACT Bayat, Klaten, Central Java, is one of three locations in Java with complete types of rocks exposed at the earth's surface. All those rocks are scattered over a short distance in Bayat, revealing past processes of rock deformation (folding, fracturing, and faulting) and present-day processes of rock weathering and erosion. In this study, we present how clastic carbonate rock of the Oyo Formation at northern Jiwo Hills could be separated about ±15 km northern from its platforms as an indication of thrust fault growth. This study uses aerial photography for photogrammetry (drones) combined with structural geology and microfossil analyses (to know the exact formation) from the outcrop observation. Recent studies have certified that drones are one reliable observation tool in various aspects with better resolution, especially in structural geology studies. Aerial photogrammetry is very well done to see the exact condition of a wide area combined with high resolution on an outcrop scale. The result shows that the carbonate rocks are from Oyo Formation (N9–N11) with the Middle Neritic bathymetric zone. The structural geology phenomenon kinematically indicates the impact of the transpressional movement called flower structure. Based on subsurface interpretation, the authors hypothesize this area was the product of an imbrication thrust stack uplifted basement as the result of the thrust fault rather than horst or paleo-basement high.

Riset Geologi dan Pertambangan
Indonesian Journal of Geology and Mining
Vol.32, No 2 pages 135–149

doi:
10.14203/risetgeotam2022.v32.1218

Keywords:
Bayat,
Oyo Formation,
thrust fault,
photogrammetry

Corresponding author:
Ardhan Farisan
Email Address: ardh005@brin.go.id

Article history
Received: 22 August 2022
Revision: 17 October 2022
Accepted: 22 November 2022

INTRODUCTION

The physiographic zones in Java recognized by van Bemmelen (1949) were identified by their structural units. The structural unit was broadly parallel to the east-west elongation of the island and the strike of the subduction trench south of Java. Van Bemmelen recognized some deformation on Java, and although it is sometimes difficult to interpret his ideas in terms of modern tectonic processes, van Bemmelen saw deformation as predominantly vertical responses to magmatic growth of geanticlinal features, which could result in thrusting and folding due to gravity-driven movements (van Bemmelen, 1949 and Clements et al., 2009).

Foreland fold-thrust belts are the most common way to accommodate crustal shortening in the frontal parts of orogens. Such belts are distributed worldwide and typically involve basement rocks and overlying sedimentary cover rocks deposited in rift and shelf basins of former continental margins (Poblet and Lisle, 2011).

The southern mountains develop a fault structure of a thrust fault as the boundary of the northern zone (Volcanic Arc of Java). According to Hall, a thrust fault in the south part of Java has displaced Paleogene volcanic arc rocks to the north for more than 50 km, and to the east, this fault distance has been reduced to 10 km (Hall et al., 2007).

In the Northern West Jiwo Hills, Bayat, volcanic, sedimentary, and metamorphic rocks are exposed at the earth's surface. All those rocks are scattered over a short distance in Bayat, revealing past processes of rock deformation (folding, fracturing, and faulting) and present-day processes of rock weathering and erosion (Bothé, 1929).

In this study, we present how the clastic carbonate rock of the Oyo Formation at northern Jiwo Hills could be separated about ±15 km northern from its platforms and bring the older rock to the top of the Oyo Formation as an indication of thrust fault growth. According to Fossen (2010), thrust faults bring older rocks on top of younger rocks and rocks of higher metamorphic grade on top of younger rocks. This study uses aerial photography for photogrammetry (drones) combined with outcrop data and microfossil analyses. As remote sensing analysis, we use BING as a resource aerial map regional–scale reference data in QGIS software, model, and regional data (previous study). Nowadays, drones are one reliable observation tool in various aspects with better resolution, especially in structural geology studies. Aerial photogrammetry is very well done to see the exact condition of a wide area combined with detailed smartphone photogrammetry with high resolution on an outcrop scale (Corradetti et al., 2021).

REGIONAL GEOLOGY

The Java island is part of an island arc formed above the north-dipping subduction zone and forms the boundary of the Indian-Australia and Eurasian (Sundaland) plates (Katili, 1975; Hamilton, 1979). Based on Hall (1996 and 2002), the thrusting age is Early Miocene or younger, but the exact age and the sequence of thrusting episodes still need to be discovered due to the absence of critical dates at thrust contact. The possibility is only to determine rock with older age than the Early Miocene have been thrusting. An Early Miocene age could indicate that thrusting is linked to the termination of the Paleogene phase of arc activity on Java. In the Early Miocene, regional plate reorganization occurred following the Australian continental collision in Eastern Indonesia, which is suggested to have initiated the counter-clockwise rotation of Borneo and Java. It contributed to the cessation or diminution of arc volcanic activity from Java eastwards in the Sunda Arc (Hall, 1996; Macpherson and Hall, 1999).

More than 100 years ago, studies of thrust systems established that thrust systems typically display a stacking order over geologic time scales with thrusts younging toward the foreland, producing the characteristic piggyback style of thrust development in time (Boyer & Elliott, 1982; Elliott, 1983).

Based on Bothé (1929), Jiwo Hills lithostratigraphically can be divided into three rock units, namely (1) Pra-Tertiary metamorphic rocks, (2) Gamping – Wungkal Formation, and (3) Oyo Formation (Figure 1). Based on SSI 1996 nomenclature compiled from Setiawan (2000), Surono et al. (1992), and Soesilo et al. (2020), the crystalline rock at West Jiwo Hills is to be Bayat Phyllite Lithodemic, Bayat Gabbro Lithodemic, and Bayat Basalt Lithodemic. Phyllite Lithodemic consists of phyllite, schist, serpentinite, and marble. Phyllite is the most important metamorphic rock at Jiwo hills, exposed at Konang hills and Semangu hills. Schist is exposed at Padasan hills at East Jiwo. Although it is not exhaustive, and marble is the lense of phyllite, it is exposed in the Jokotuo hills. In phyllite lithodemic, there is no fossil appeared, so the specific age of phyllite is unknown because Tertiary-aged formation covered phyllite. The age of phyllite is set in pre-Tertiary.

Based on the seismic interpretation of East Java and projected to the Bayat area (Prasetyadi, 2007), in Figure 2, Bayat is interpreted as a paleo-basement high or horst. In this interpretation, this paleo-basement high or horst causes exposure of pre-tertiary rocks or basements in Bayat. We will discuss further explanations in the results and discussion sub-chapters.

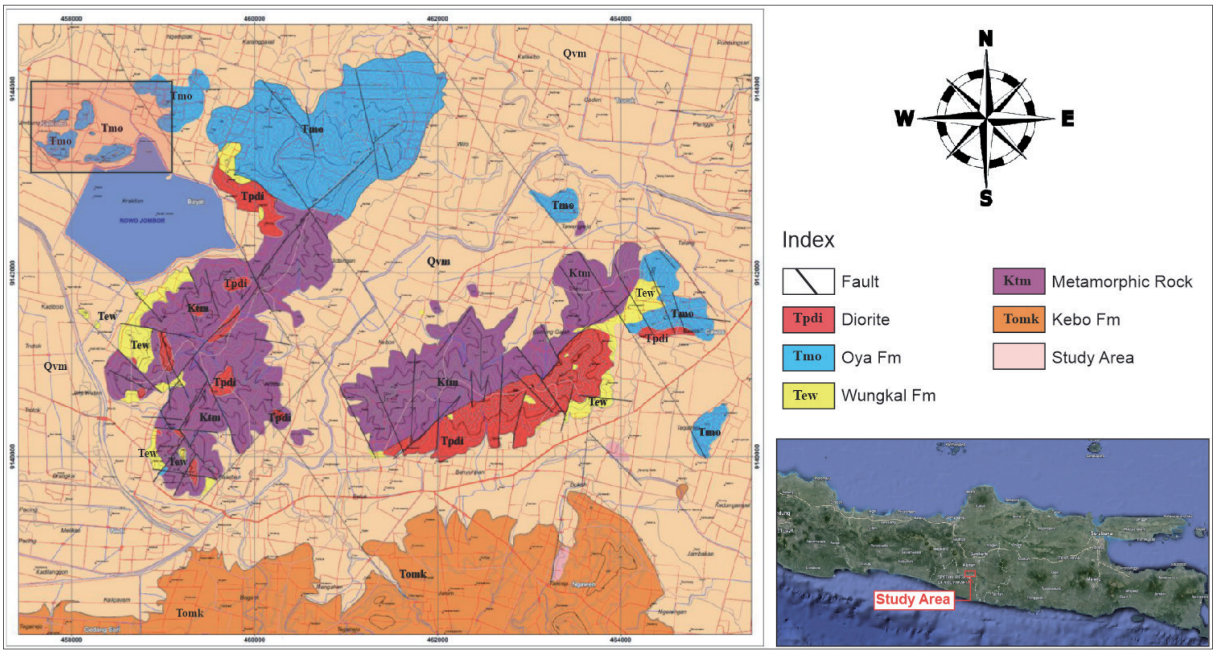

Figure 1. Geological map of Jiwo Hill, Bayat, Klaten. Compiles from Surono et al. (2009) and Soesilo et al. (2020).

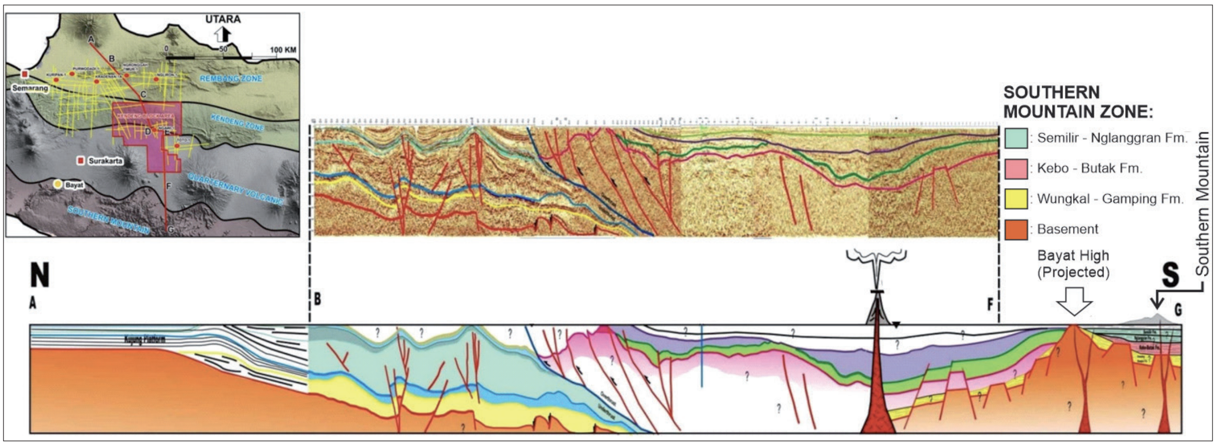

Figure 2. Structural style interpretation of Eastern Java using a seismic image. This figure showing Bayat/ Jiwo Hill area is a horst or paleo-basement high (Prasetyadi, 2007).

METHODOLOGY

Limitations in interpreting geological structures are an obstacle for geoscientists because the range of observation needs to be bigger to observe the continuity, straightness, and geometry characteristics. Using UAVs, we can take a broader look at the feature of geological structures. In this study, research was carried out by integrating extensive field studies. The methodology in this research is mainly field-based research with few tools and studio interpretation using QGIS as remote sensing software and photogrammetry processing software. The fieldwork tools use aerial photography (drones) to see widely structural and lithology from above, outcrop analyses (especially for structural geology interpretation), and rock sampling for age determination.

Photogrammetry

Recent studies have certified that the accuracy of the image-based models from a photogrammetric assembly of a set of overlapping photographs equals or is comparable to the accuracy of models produced by LIDAR-based construction (Adams and Chandler, 2002; Harwin and Lucieer, 2012). The photo-based 3D reconstruction method is the evolution of photogrammetry with a unique technique that does not require expensive hardware and high accuracy. Fundamentally, photogrammetry works by overlapping several photos (Figure 3). The series of images can overlap and make 3-dimensional (3D) resolution photos. Some pictures are given coordinates as connecting points in georeferencing (Bemis et al., 2014). This photo data can be taken using a digital camera or UAV (Unmanned Aerial Vehicle). Based on Vollgger & Cruden (2016), The research on aerial photogrammetry on the folds and fractures can produce statistical data on spread & fracture trends and fold trends, types & axes to fold reconstruction. Studies of various scales try to identify values of the same stocky density at regional scales, outcrops, or thin cuts. Various studies explain some perspective errors because they focus specifically on outcrops that have flat surfaces.

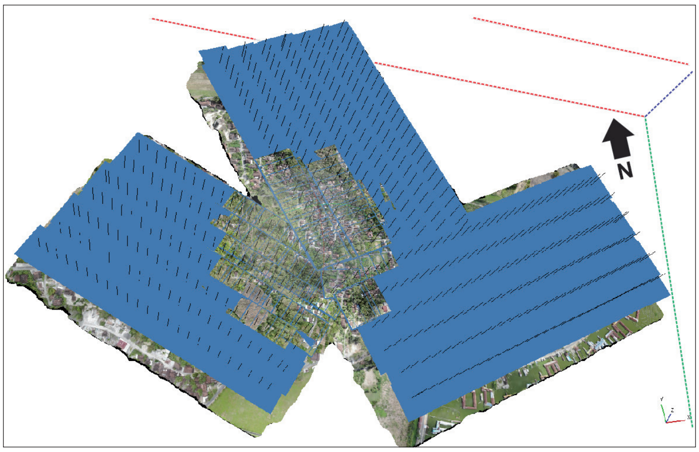

Figure 3. Photography acquisition perspective.

The main steps of the photogrammetry method (Menegoni et al., 2019; Inama, Menegoni & Perotti, 2020), as seen in Figure 4, require (1) data acquisition: collected images, both aerial and land acquisition. Dronedeploy software could provide acquisition aerial photography automatically with GPS onboard position in every shot. 75% overlapping in every image is required for the best result. All images were georeferences using the coordinates registered by onboard GPS. The specification of the drone camera can be seen in Table 1.

Table 1. Camera hardware specifications.

Hardware	Sensor	Lens
DJI Mavic Air	Effective: 12 MP FOV: 85° 35 mm EQ 24 mm	Aperture: f/2.8 SR: 0.5 to ∞

(2) Data processing requires: (a) image matching and creation using high accuracy (complete resolution matching) pre-selection method; (b) dense Computer creation as high-quality parameters of photoscan procedures generates ± 73 million points at the end of the process; (c) mesh creation with all parameters using suggested by the software; (d) texture mapping generates generic texture mapping, and mosaic blending is used to obtain the texture for the mesh by default of software with a quality value of 0.7; (e) extracting data/ export tiff (image and DTM model data) using the WGS84 metric coordinate system and integrating with terrain data from BING Satelite in QGIS.

(3) Model interpretation requires regional geology data and previous studies to support research data. The data needed are regional geological maps compiled from Surono et al. (1992) and Soesilo et al. (2020) and remote sensing using the BING satellite, which is extrapolated to data due to the limitations of data acquisition using UAV. This interpretation then uses kinematic analysis to determine the type of fault. After the kinematic analysis is carried out, the next step is to make a subsurface interpretation.

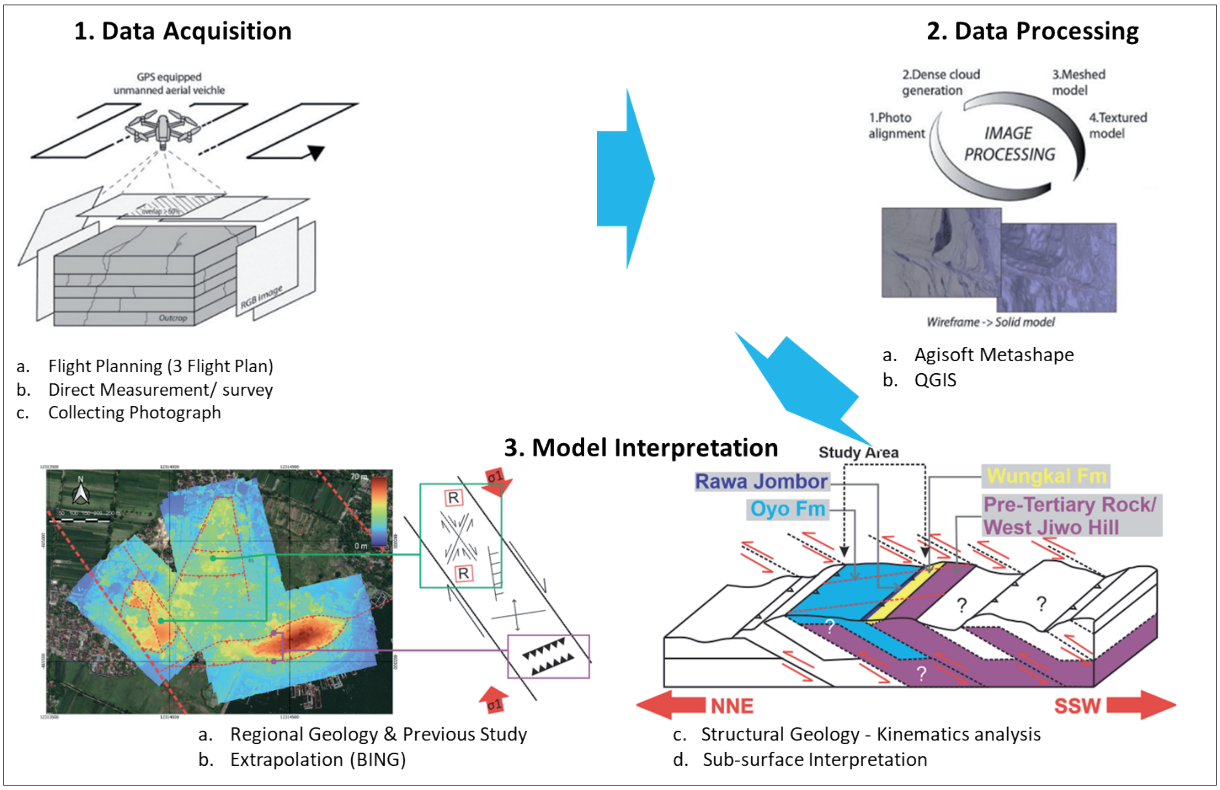

Figure 4. Schematic workflow followed for generating photogrammetry model and integrating with essential data. Modified from Innama et al. (2020).

Micropaleontological analyzes

A micropaleontological analysis is required to know the exact formation in this area. The main steps of the micro-paleontological analysis method are: (1) field sampling from the massive sedimentary structure and bedding structure and (2) preparing the sample, cleaning the sample and removing burial matter, (3) observation and description of foraminifera to identify age using Blow (1969), (4) sorting and counting foraminifera abundance to identify bathymetric zone using Barker (1960).

GIS and regional analyzes

GIS and regional analyzes requiring steps: (1) Import data from Agisoft such as tiff from orthophoto and D.T.M. (Digital Terrain Model). (2) Identifying and interpreting structural items such as lineation, fault, and fracture. (3) Overlaying orthophoto with regional aerial data using BING satellite images. (4) Overlaying images with regional geology and previous study data (Surono et al., 1992; Soesilo et al., 2020).

RESULTS

Aerial photogrammetry

This study uses aerial photogrammetry to determine and interpret structural geology. Study reference using the Geological Map of Jiwo Hill, Bayat, Klaten (Surono et al., 1992; Soesilo et al., 2020) in Figure

1 shows the study area inside the two lineations we interpreted as a structural boundary. We divided this section into three regions (north, west, and south). The section is divided by the range of drone collection data and structural geology, as seen in Figure 5. The characteristics of structural geology in every area are slightly different. The result from aerial photogrammetry can be seen in Table 2.

Table 2. Aerial photogrammetry result

PARAMETER	Photo	Dense Cloud	Tiled Model	DEM	Orthomosaic	Area
RESULT	504	73,146,438	9 levels	13.700 x 10.898	40.216 x 28.220	60
	photos	points cloud	3.21 cm/pix	12.9 cm/pix	3.21 cm/pix	hectares

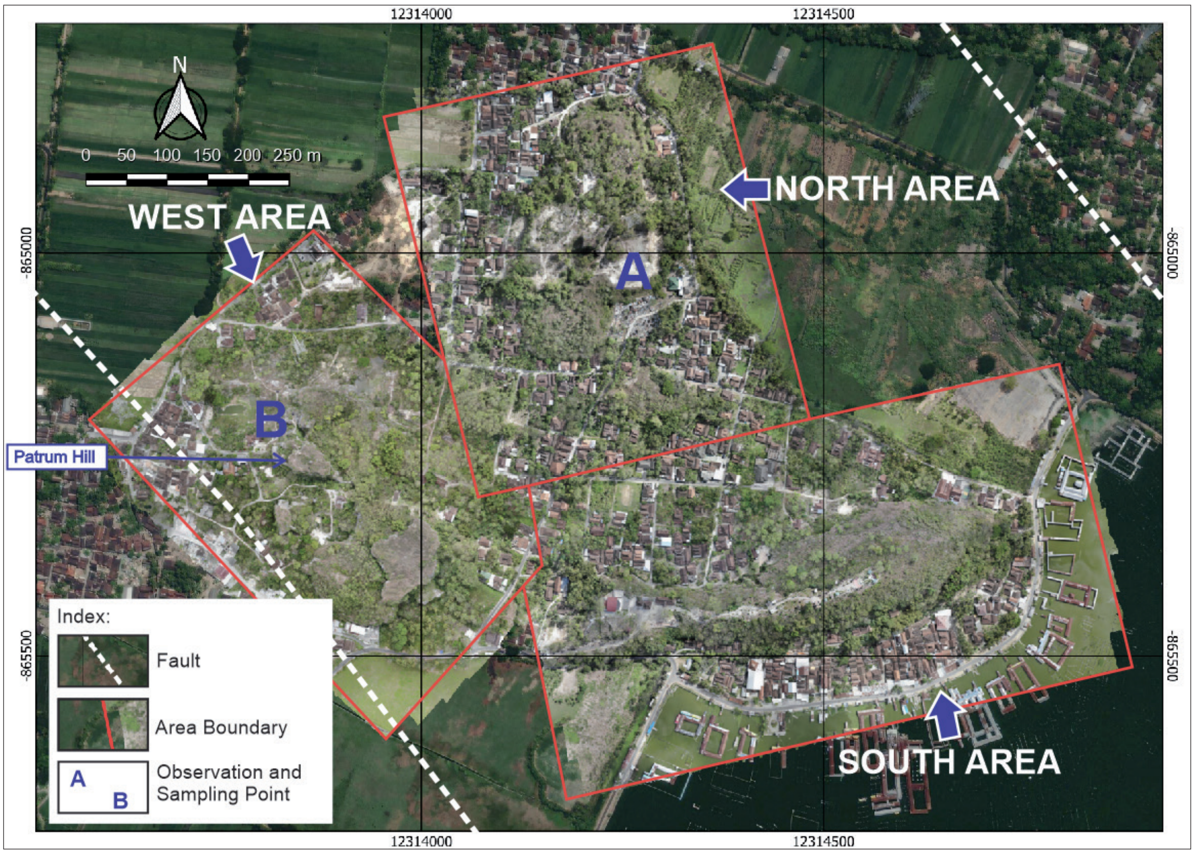

Figure 5. Area and rock sampling & fault analyzes location. Structural map reference: compiled from Surono et al. (1992) and Soesilo et al. (2020).

A. North area

We interpreted the north area as a flower structure product. The north area has an axis of elongation with direction N010°E. Flower structures are typical for wrench fault zones and have usually been considered one of the essential features used to identify strike-slip faults in regional tectonic studies (Christie-Blick & Biddle 1985). The carbonate rock in the north area is bounded by two (2) faults lineation that is relatively popping up with the direction of NNE–SSW at the west and NNW–SSE at the east. This fault movement growth results in two (2) reverse faults with relatively W–E direction in the northern area.

In Figure 6, Bird-eye 1 shows the range of three (3) reverse faults with a dip direction to the south. Bird-eye 2 shows that the major fault is a boundary of the carbonate rock region. This range of faults was responsible for pop-uping rock in this area. Further analysis will be elaborated in the structural geology and kinematics chapter.

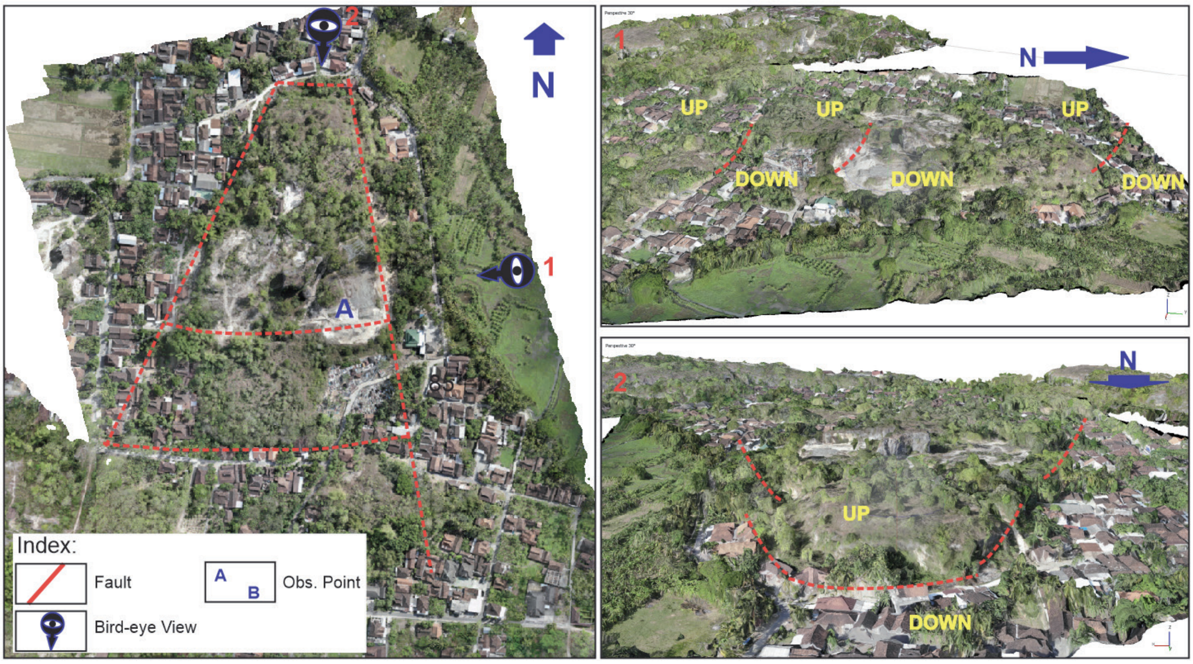

Figure 6. Left: aerial photogrammetry of the north area. Upper Right: aerial view from bird-eye 1. Lower Right: aerial view from bird-eye 2.

The aerial photogrammetry shows that the north area consists of lineation from fault growth with a direction of W–E. This structure believes to have formed from the development of the thrust belt. The fault plane has N095°E/42° and rakes: 74° (Figure 7). Based on Rickard (1972) in Figure 8, the fault name is the left reverse thrust fault.

Figure 7. Outcrop photo of the North section showing growth of reverse fault.

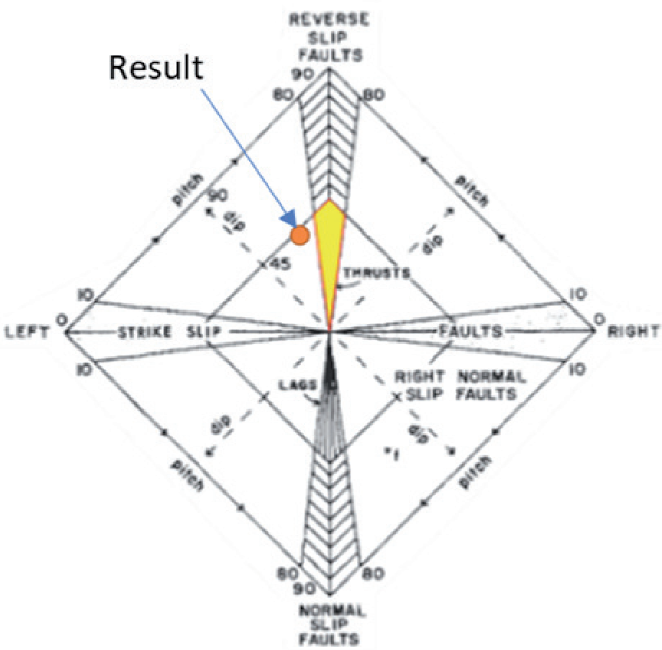

Figure 8. Fault classification by Rickard (1972).

B. West area

The west area has a more complex structure growth. The structure growth is from the major structure (Figure 9). Based on Surono et al., 1992, and Soesilo et al., 2020, there is a structure at the SW with a relatively NW–SE direction. In bird-eye 3 and 4, we see many minor faults with broad orientations inside this fault zone. The reverse fault inside the zone has a relatively NNE–SSW direction and strike-slip fault from NW–SE, W–E, and N–E.

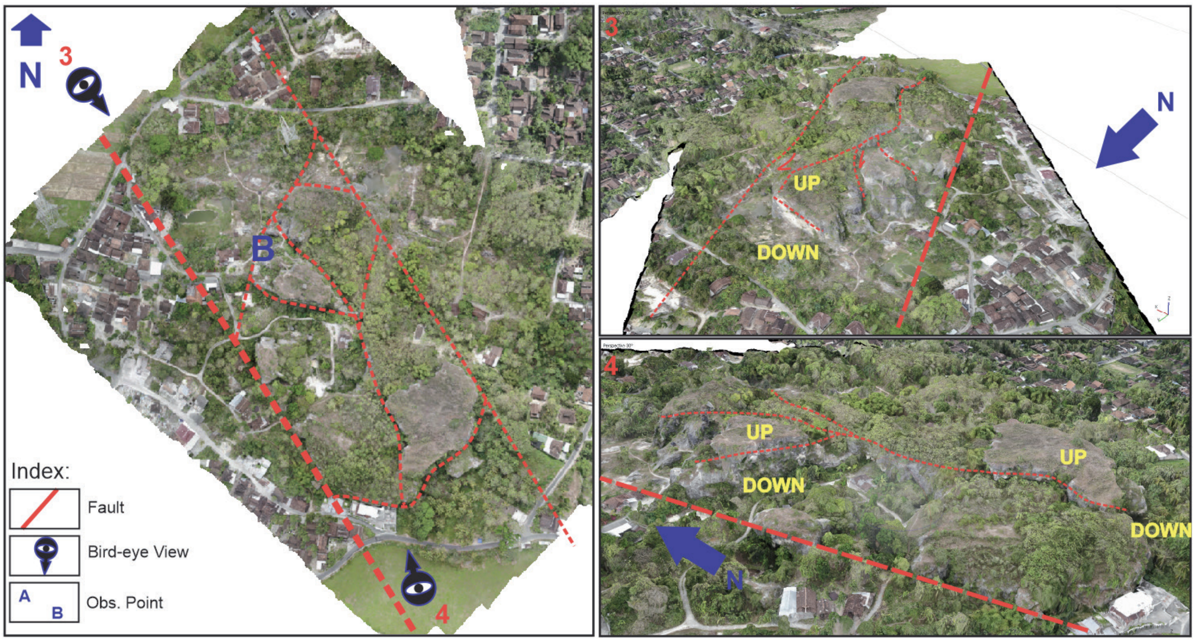

Figure 9. Left: aerial photogrammetry of the West Area. Upper right: aerial view from bird-eye 3. Lower right: aerial view from bird-eye 4.

Bayat is known as an area with Pre-Tertiary, Eocene, to Oligocene age rocks, so it will be a question for carbonate rocks to be found in this area. According to Surono (2009), the carbonate period started in the Middle of the Miocene to Pliocene. We use fossil analysis to determine the exact formation. The analysis consists of planktonic foraminifera for the age of deposition and benthic foraminifera for the bathymetric depositional environment. Rock sampling was taken from two (2) types of sedimentary structures, (A) massive and (B) cross-bedding sedimentary structures, for more accurate analysis (Figure 10). The massive sedimentary structure has a bedding plane of N078°E/24° while the cross-bedding of N122°E/47°.

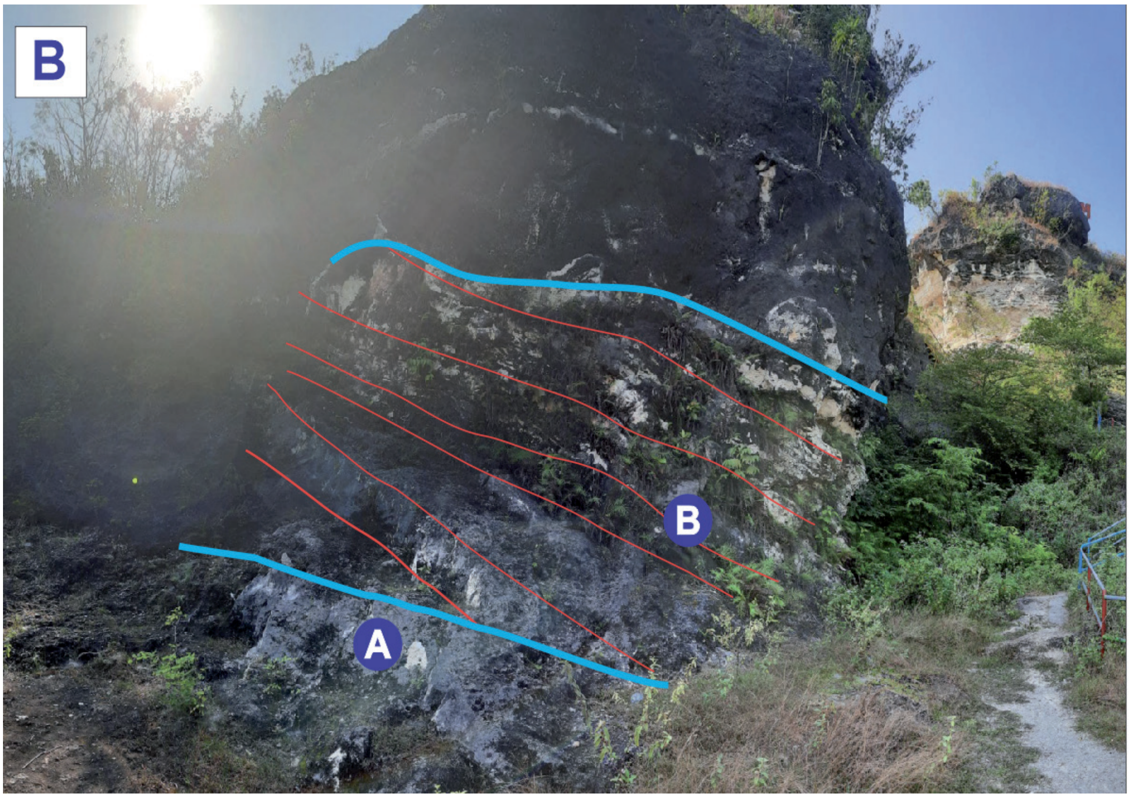

Figure 10. The sampling point in the west area (observation point B): (A) a massive sedimentary structure and (B) a cross-bedding sedimentary structure.

(A) Massive sedimentary structure

This analysis found ratio abundance of fossils is medium range, with a 50%–26% ratio between plankton and benthos. After we describe and interpret the age using Blow (1969), it can be determined that the absolute age of this sample is N10–N11, which is in the Middle Miocene ages. Further details can be seen in Table 3. Based on benthic foraminifera analyses by Barker (1960), we can conclude that the bathymetry environment is in Middle Neritic (Table 4).

Table 3. Planktonic foraminifera analytic in massive sedimentary structure.

No	Planktonic Foraminifera Species	Abun-dance	Geological Time Scale (Blow, 1969)																						
			Oligocene			Miocene														Pliocene			Plisto-cene		
						Early					Middle						Late			Early		Late			
			P20/ N1	P21/ N2	P22/ N3	N4	N5	N6	N7	N8	N9	N10	N11	N12	N13	N14	N15	N16	N17	N18	N19	N20	N21	N22	N23
1	*Globigerina venezuelana*	M																							
2	*Globorotalia praemenardii*	M																							
3	*Globigerina juvenilis*	M																							
4	*Globigerinoides altiaperturus*	M																							
5	*Globigerina druryi*	M																							
6	*Orbulina bilobata*	M																							
7	*Orbulina universa*	M																							
8	*Globigerinoides sacculifer*	M																							

Table 4. Benthic foraminifera analytic in massive sedimentary structure.

Barker, 1960										
No	Benthic Foraminifera Species	Abun-dance	Transition	Neritic			Bathyal		Abyssal	Hadal
				Upper	Middle	Lower	Upper	Lower		
			0	20	100	200	500	2000	4000	
1	*Conorboides advena (29,28-45,75 m)*	M								
2	*Protoschista findens (32,94-36,6 m)*	M								
3	*Bigenerina cylindrica (82,35-109,8 m)*	M								
4	*Discorbis sp. (69,54-73,2m)*	M								
5	*Textularia pseudogarmen (69,54-73,2m)*	M								
6	*Heronallenia lingulata (69,54-73,2m)*	M								

(B) Cross-bedding sedimentary structure

This analysis found ratio abundance of fossils is medium range, with a 50%–26% ratio between plankton and benthos. After we describe and interpret the age using Blow (1969), it can be determined that the absolute age of this sample is N9–N10 (Middle Miocene). Further details can see in Table 5. Based on benthic foraminifera analyses by Barker (1960), we can conclude that the bathymetry environment is in the middle neritic (Table 6). Based on the analysis and Surono (2009), it can be supposed that the lithology in this study area is Oyo Formation with an age range of N9–N11 or Middle Miocene (Figure 11).

Table 5. Planktonic foraminifera analytic in cross-bedding sedimentary structure.

No	Planktonic Foraminifera Species	Abun-dance	Geological Time Scale (Blow, 1969)																						
			Oligocene			Miocene														Pliocene				Plisto-cene	
						Early					Middle						Late			Early		Late			
			P20/ N1	P21/ N2	P22/ N3	N4	N5	N6	N7	N8	N9	N10	N11	N12	N13	N14	N15	N16	N17	N18	N19	N20	N21	N22	N23
1	*Globigerinoides altiaperturus*	M																							
2	*Globigerinoides obliquus*	M																							
3	*Globigerinoides trilobus*	M																							
4	*Globigerinita incrusta*	M																							
5	*Globorotalia praescitula*	M																							
6	*Orbulina universa*	M																							
7	*Globigerinoides subquadratus*	M																							
8	*Globoquadrina obessa*	M																							

Table 6. Benthic foraminifera analytic in cross-bedding sedimentary structure.

Barker, 1960										
No	Benthic Foraminifera Species	Abun-dance	Transition	Neritic			Bathyal		Abyssal	Hadal
				Upper	Middle	Lower	Upper	Lower		
			0	20	100	200	500	2000	4000	
1	*Buccella frigida (100,65m)*	M								
2	*Discorbis australis (68,54 - 73,2)*	M								
3	*Cancris indicus (67,71m)*	M								
4	*Neoconorbina terquemi (32,94m)*	M								
5	*Rosalina sp. (27,45m)*	M								
6	*Anomalinella rostrata (67,71m)*	M								

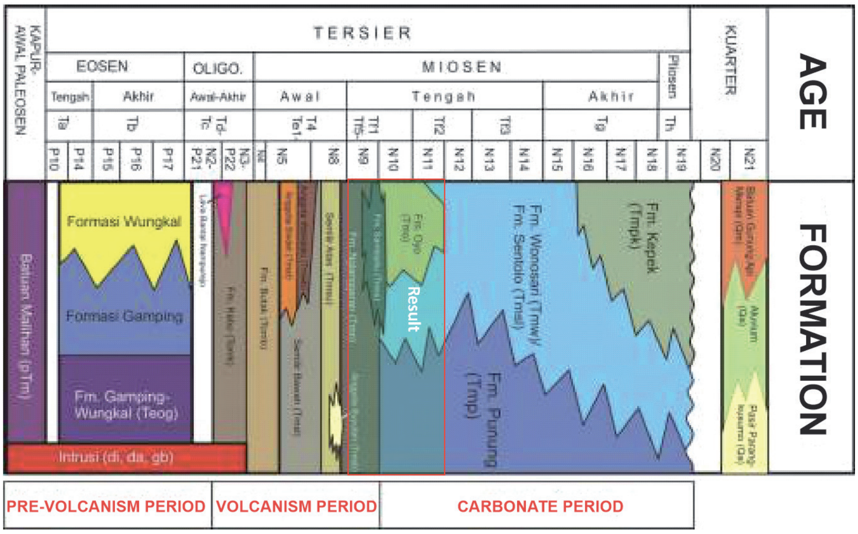

Figure 11. Stratigraphy of the west part of the Southern Mountain (Surono, 2009).

C. South area

The south area has a simpler structure, as seen above (Figure 12). There is a poping-up zone inside of the reverse fault boundary. The direction of this reverse fault is relatively ENE–WSW with a dip direction to NNW and SSE. In the southern part of this structure is a lake known as the Jombor Swamp. This study proves that the Jombor Swamp results from a basin produced by piggybacks from a thrust fault. Further elaboration (kinematics and sub-surface interpretation) will be in the discussion chapter.

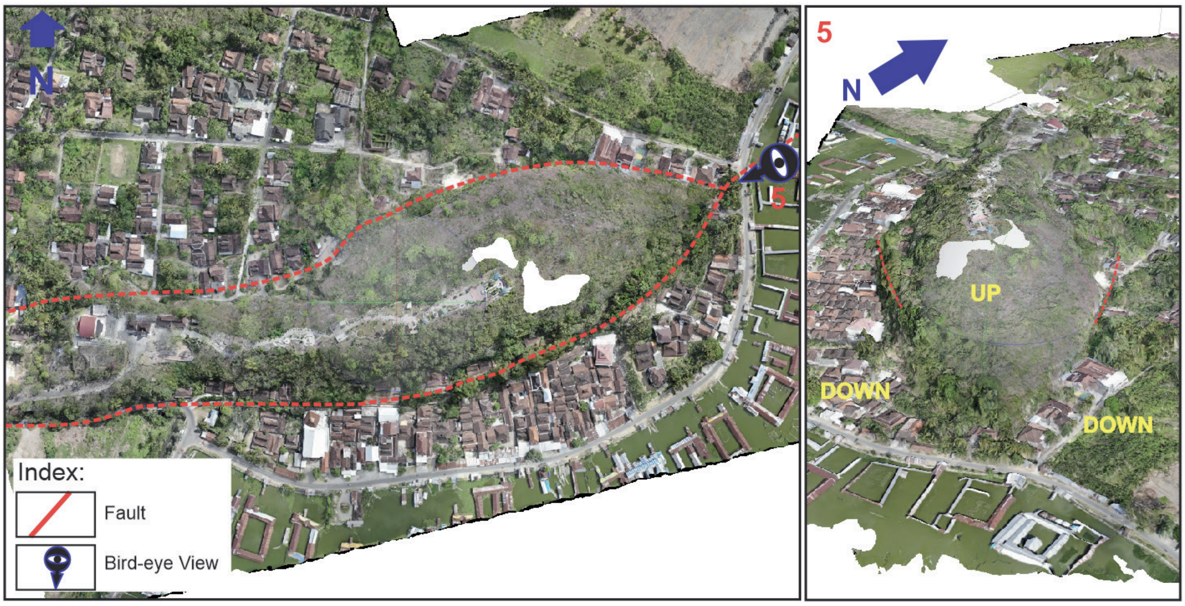

Figure 12. Left: aerial photogrammetry of the east area. Right: aerial view from bird-eye 5

DISCUSSION

Structural geology & kinematics

This sub-chapter used Digital Terrain Model (DTM) extracted from photogrammetric data (tiled model) for interpreting purposes. Kinematics determines how the structure in the strike-slip fault zone is formed. In this study, we interpret the strike-slip zone using a transpressional model of Sanderson & Marchini (1984). Based on the regional geology map by Surono et al. (1992) and Soesilo et al. (2020), the area of study is bounded by two (2) lineation with the direction of NW–SE movement, producing some fault blocks that have transformed, up, and offset.

The fault block movement is called flower structure. These flower structure features are mainly characterized by their internal fault and fold architecture and their association with straight and continuous deformation zones. In conventional models, flower structures are classified into two types according to their internal structural architecture: positive and negative (Harding, 1985 and 1990).

Figure 13 shows the structure of the north and west area using the Digital Terrain Model (DTM) is expected to form from the development of Riedl shear. The south area was slightly different, developed from the reverse fault movement inside flower structure zones. Based on Sanderson & Marchini (1984), the geometry and kinematics of structures expected for this study area are controlled by a maximum compression ($\sigma1$) axis in an approximately NNW–SSE.

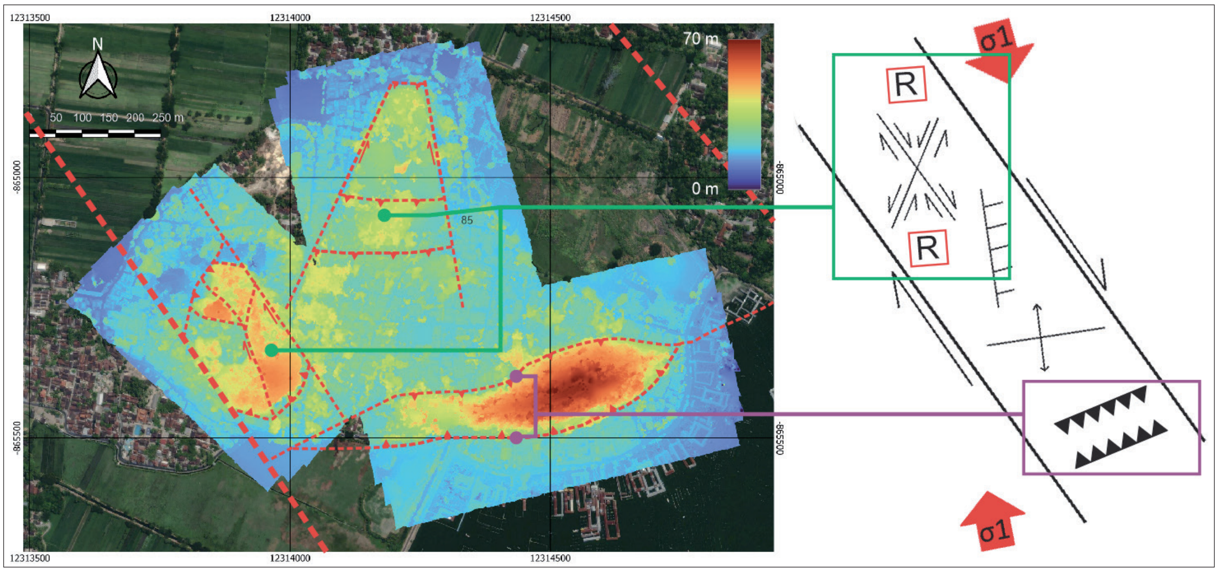

Figure 13. Digital Terrain Model (DTM) of the study area showing transpressional deformation according to the strain model of Sanderson and Marchini (1984)

Sub-surface interpretation

In this section, we overlay a regional geological map of Surono et al. (1992) and Soesilo et al. (2020) and photogrammetry results from our study using QGIS software (figure 14). The study area consists of metamorphic rock (Pre-Tertiary) and Tertiary rock such as Wungkal Formation, Oyo Formation, and Diorite intrusion. Based on Surono et al. (1992) and Soesilo et al. (2020), The East Jiwo Hills complex areas show the main direction of the NW-SE structure with some minor structures with the SW–NE and W–E directions. The study area was in the major lineage with the direction of NW–SE. We made a cross-section in the direction of NW–SE considering that the cross-section is in the major structure (NW–SE).

The cross-section interpretation in Figure 15 shows that the older rock (metamorphic rock) is on top of the younger rock (carbonate of Oyo Formation) due to thrust fault growth. The structural geology analysis in the study shows a stacking system called an imbrication thrust stack (Whittington, 2004). This phenomenon causes the exhumation and uplifting of West Jiwo Hills (Figure 16). This study proves that the Jombor Swamp results from a basin produced by piggybacks from a thrust fault. The authors hypothesize that this area was a tectonic uplifted basement rather than a horst/paleo-basement high.

The results obtained from the kinematic analysis show that the study area, which is the carbonate of the Oyo Formation, is the product of the transpressional system. However, when the author uses a broader scale by identifying that the Oyo Formation carbonate can be separated ±15 km from its platform in the southern mountains as a product of the imbricated thrust stack, it will be fascinating for further research to find a relationship between the transpressional system and the imbricated thrust stack.

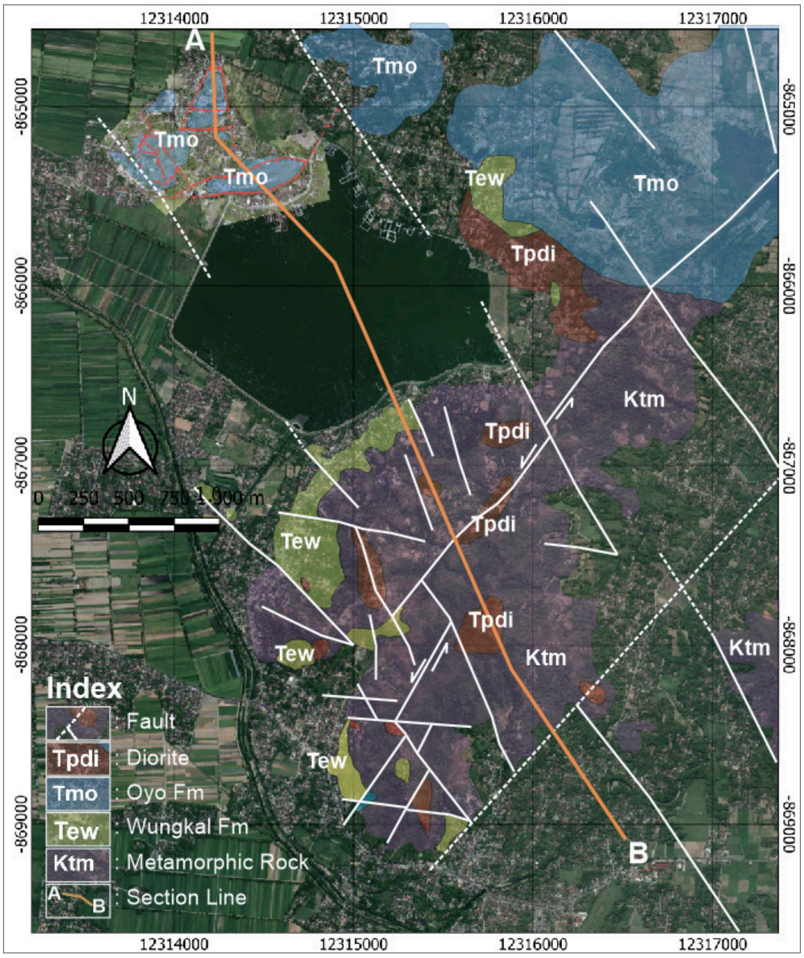

Figure 14. The study area overlays with the geological map by Surono et al. (1992) and Soesilo et al. (2020).

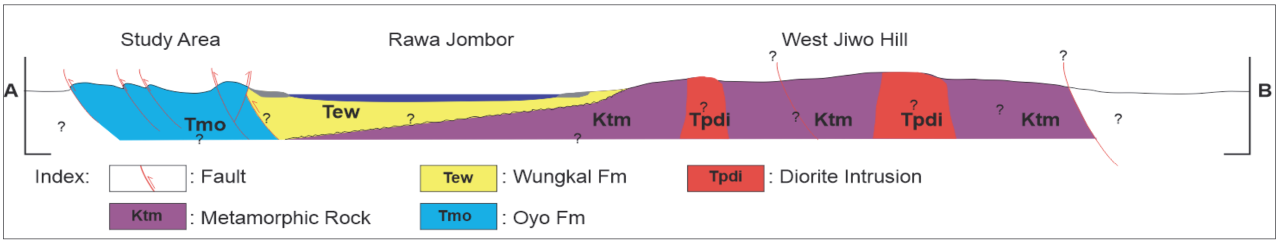

Figure 15. The interpretation of the cross-section of the study area shows a growth of the thrust belt.

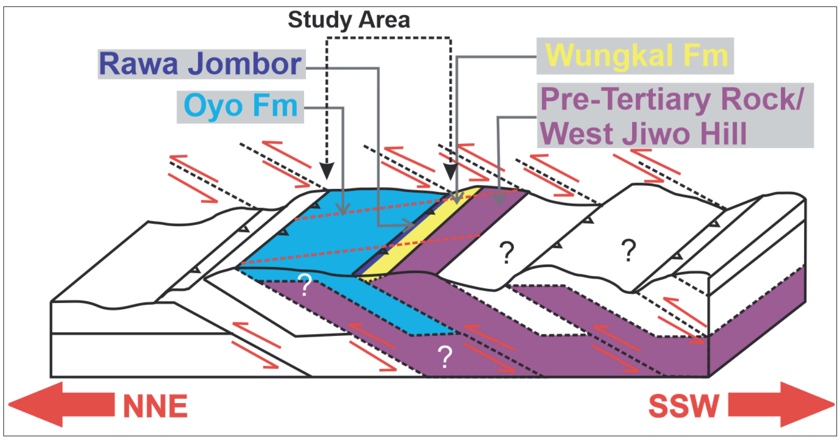

Figure 16. Modified imbricate thrust stack model by Whittington (2004) as a suggested model to explain the exhumation of West Jiwo Hills, Bayat. This model also proves that Jombor Swamp was a piggyback product of thrust fault.

CONCLUSIONS

The result of aerial photogrammetry shows a dense cloud with 73,146,438 points cloud, a tiled model with 9 levels and 3.21 cm/pix, and a DEM with 13.700 x 10.898 points with 12.9 cm/pix, orthomosaic 40.216 x 28.220 points with 3.21 cm/pix, and area 60 hectares. The interpretation results in the north area: the carbonate rock in the north area is bounded by two lineations that are relatively popping up with the direction of NNE - SSW at the west and NNW - SSE at the east. The fault plane has N095°E/42° and rake 74°, named left reverse thrust fault. West area: inside the lineation (NW–SE) fault zone are many minor faults with broad directions. The reverse fault inside the zone has a relatively NNE - SSW direction and strike-slip fault from NW–SE, W–E, and N–E. East area: the direction of popping up the reverse fault is relatively ENE–WSW with a dip direction to NNW and SSE. Based on microfossil analytics, the bathymetry of this area of study is in Middle Neritic (50% - 26% ratio between plankton and benthos) with an age of absolute range N9 - N11 (Middle Miocene) in Oyo Formation. Kinematics result in the structure growth of this study area being impacted by transpressional movement. The transpressional movement has produced blocks developed from Riedl shear called flower structures. The structural geology analysis in the study shows that a stacking system called imbrication thrust stack causes the exhumation and uplifting of West Jiwo Hills, and the Jombor Swamp results from a basin produced by piggybacks from a thrust fault. The authors hypothesize this area was a tectonic uplifted basement rather than a paleo-basement high or horst.

REFERENCES

Adams, J., Chandler, J., 2002. Evaluation of lidar and medium-scale photogrammetry for detecting soft-cliff coastal change. Photogramm. Rec. 17, 405e418.

Barker, R. W., 1960. Taxonomic notes on the species figured by H.B. Brady in his report of the foraminifera dredged by HMS Challenger during the years 1873-1876. SEPM Special Publication. 9: 1-238.

Bemis, S. P., Micklethwaite, S., Turner, D., James, M. R., Akciz, S., T. Thiele, S., & Bangash, H. A., 2014. Ground-based and UAV-Based photogrammetry: A multi-scale, high-resolution mapping tool for structural geology and paleoseismology. Journal of Structural Geology, 69(PA), 163–178. https://doi.org/10.1016/j.jsg.2014.10.007

Blow, W.H., 1969. Late Middle Eocene to Recent Planktonic Foraminiferal Biostratigraphy. In: Bronnimann, P. and Renz, H.H., Eds., Proceedings of the 1st International Conference on Planktonic Microfossils, Geneva, Vol. 1, 199-422.

Bothé, A.Ch.D., 1929. Jiwo Hills and Southern Range Excursion Guide. IVth Pacific Science Congress, Java, Bandung, pp. 1-14.

Boyer, S.E., Elliott, D., 1982. Thrust systems. American Association of Petroleum Geologists Bulletin 66, 1196-1230.

Christie-Blick, N., & Biddle, K. T., 1985. Deformation and basin formation along strike-slip faults. In K. T. Biddle & N. Christie-Blick (Eds.), Strike-slip deformation, basin formation, and sedimentation. Society of Economic Paleontologists and Mineralogists Special Publication, 37, 1– 34.

Clements, B., R. Hall, H. R. Smyth, and M. A. Cottam, 2009. Thrusting of a volcanic arc: A new structural model for Java, Pet. Geosci., vol. 15, no. 2, pp. 159–174, DOI: 10.1144/1354-079309-831.

Corradetti, A., Seers, T. D., Billi, A., Tavani, S., 2021. Virtual Outcrops in a Pocket: The Smartphone as a Fully Equipped Photogrammetric Data Acquisition Tool. The Geological Society of America (GSA) Today. http://dx.doi.org/10.1130/GSATG506A.1

Elliott, D., 1983. The construction of balanced cross-sections. Journal of Structural Geology 5, 101.

Fossen, H., 2010. Structural Geology. Cambridge University Press, New York. 313p.

Hall, R., 1996, Reconstructing Cenozoic SE Asia, in Hall, R., and Blundell, D.J., eds., Tectonic Evolution of SE Asia, Geological Society of London Special Publication, v. 106, p. 153-184.

Hall, R., 2002, Cenozoic geological and plate tectonic evolution of the SE Asia and the SW Pacific: computer-based reconstruction, model and animations, Journal of Asian Earth Sciences, v. 20, p. 353-434.

Hall, R., Clements, B., Smyth, H.R., dan Cottam, M.A., 2007. A new interpretation of Java's structure, Proceedings Indonesian Petroleum Association, 31st Annual Convention.

Hamilton, W., 1979. Tectonics of the Indonesian region. United States Geological Survey Professional Paper, 1078pp.

Harding, T. P., 1985. Seismic characteristics and identification of negative flower structures, positive flower structures, and positive structural inversion. AAPG Bulletin, 69, 585– 600.

Harding, T. P., 1990. Identification of wrench faults using subsurface structural data: Criteria and pitfalls. AAPG Bulletin, 74, 1590– 1609.

Harwin, S., Lucieer, A., 2012. Assessing the accuracy of georeferenced point clouds produced via multi-view stereopsis from unmanned aerial vehicle (UAV) imagery. Remote Sens. 4, 1573-1599.

Katili, J.A., 1975. Volcanism and Plate Tectonics in the Indonesian Island Arcs. Tectonophysics, 26, p.165-188. DOI: 10.1016/00401951(75)90088-8

Macpherson, C.G., and Hall, R., 1999, Tectonic controls of geochemical evolution in arc magmatism of SE Asia, Proceedings 4th PACRIM Conference, Australian Institute of Mining and Metallurgy, p. 359-368.

Menegoni, D. Giordan, C. Perotti, and D. D. Tannant, 2018. Detection and geometric characterization of rock mass discontinuities using a 3D high-resolution digital outcrop model generated from RPAS imagery – Ormea rock slope, Italy. Eng. Geol., vol. 252, pp. 145–163, 2019, doi: 10.1016/j.enggeo.2019.02.028.

Poblet, J., Lisle, R.J., 2011. Kinematic evolution and structural styles of fold-and-thrust belts. Geol. Soc. Spec. Publ. 349, 1–24. https://doi.org/10.1144/SP349.1.

Prasetyadi, C., 2007. Evolusi Teknik Paleogen Jawa Tengah Bagian Timur. Disertasi Doktor, Institute Teknologi Bandung, 2007, (Tidak terbit); 323h.

Inama, R., N. Menegoni, and C. Perotti, 2020. Syndepositional fractures and architecture of the lastoni di formin carbonate platform: Insights from virtual outcrop models and field studies. Mar. Pet. Geol., vol. 121, no. July, 2020, DOI: 10.1016/j.marpetgeo.2020.104606.

Rickard, M. J., 1972. Fault Classification: Discussion. Geological Society of America Bulletin, v. 83, p. 2545-2546. https://doi.org/10.1130/0016-7606(1972)83[2545:FCD]2.0.CO;2

Sanderson, D.J., Marchini, W., 1984. Transpression. Journal of Structural Geology 6 (5), 449– 549.

Setiawan, J., 2000. Evolusi Struktur Perbukitan Jiwo, Bayat, Klaten, Jawa Tengah. Institut Teknologi Bandung, Tesis Magister (S2), Unpublished.

Soesilo, J., B. T. Wibowo, A. Majid, and P. Jiwo, 2020. Karakteristik dan Pembentukan Batuan Beku di Pegunungan Jiwo, Bayat, Jawa Tengah. Jurnal Mineral, Energi, dan Lingkungan vol. 4, no. 2, pp. 18–31.

Surono, 2009. Litostratigrafi Pegunungan Selatan bagian timur, Daerah Istimewa Yogyakarta dan Jawa Tengah. Jurnal Sumber Daya Geologi, 19 (3): 209-221.

Surono, Toha, B., dan Sudarno, I, 1992. Peta Geologi Lembar Surakarta-Giritontro, Jawa, Skala 1:100.000. Pusat Penelitian dan Pengembangan Geologi, Bandung.

van Bemmelen, R.W. 1949. The Geology of Indonesia. Government Printing Office, Nijhoff, The Hague.

Vollgger, S. A., & Cruden, A. R., 2016. Mapping folds and fractures in the basement and cover rocks using UAV photogrammetry, Cape Liptrap and Cape Paterson, Victoria, Australia. Journal of Structural Geology, 85, 168–187. https://doi.org/10.1016/j.jsg.2016.02.012

Whittington, A.G., 2004. The exhumation of gneiss domes in bivergent wedges: Geometrical concepts and examples from the Himalayan syntaxes. In: Whitney, D.L, Teyssier, C., Siddoway, C.S., Gneiss domes in orogeny. Geological Society of America, Special Paper 380.